



## Research Article

## Deep Transfer Learning Model for EEG Biometric Decoding

Rasha A.Aljanabi<sup>1</sup>, , Z.T.Al-Qaysi<sup>1, \*</sup>, , M. S Suzani<sup>2</sup>, <sup>1</sup>Tikrit University, College of Computer Science and Mathematics, Computer Science Department, Iraq<sup>2</sup>Data Intelligence and Knowledge Management Special Interest Group, University Pendidikan Sultan Idris, Tanjong Malim, Perak, Malaysia

## ARTICLEINFO

## Article History

Received 26 Dec 2023

Revised 17 Jan 2024

Accepted 03 Feb 2024

Published 28 Feb 2024

## Keywords

Brain-Computer  
Interface  
Motor Imagery  
Deep Learning  
Transfer Learning  
VGG-19  
Biometric  
Short-time Fourier  
transform

## ABSTRACT

In automated systems, biometric systems can be used for efficient and unique identification and authentication of individuals without requiring users to carry or remember any physical tokens or passwords. Biometric systems are a rapidly developing and promising technology domain, contrasting with conventional methods like password IDs. Biometrics refer to biological measures or physical traits that can be employed to identify and authenticate individuals. The motivation to employ brain activity as a biometric identifier in automatic identification systems has increased substantially in recent years, with a specific focus on data obtained through electroencephalography (EEG). Numerous investigations have revealed the existence of discriminative characteristics in brain signals captured during different types of cognitive tasks. However, due to their high-dimensional and nonstationary nature, EEG signals are inherently complex, requiring specialized feature extraction and classification techniques. In this study, a hybridization method that combined a classical classifier with a pre-trained convolutional neural network (CNN) and the short-time Fourier transform (STFT) spectrum was employed. For tasks such as subject identification and lock and unlock classification, we employed a hybrid model in mobile biometric authentication to decode two-class motor imagery (MI) signals. This was accomplished by building nine distinct hybrid models using nine potential classifiers, primarily classification algorithms, from which the best one was finally selected. The experimental portion of this study involved, in practice, six experiments. For biometric authentication tasks, the first experiment tries to create a hybrid model. In order to accomplish this, nine hybrid models were constructed using nine potential classifiers, which are largely classification methods. Comparing the RF-VGG19 model to other models, it is evident that the former performed better. As a result, it was chosen as the method for mobile biometric authentication. The performance RF-VGG19 model is validated using the second experiment. The third experiment attempts for verifying the RF-VGG19 model's performance. The fourth experiment performs the lock and unlock classification process with an average accuracy of 91.0% using the RF-VGG19 model. The fifth experiment was performed to verify the accuracy and effectiveness of the RF-VGG19 model in performing the lock and unlock task. The mean accuracy achieved was 94.40%. The sixth experiment validated the RF-VGG19 model on unseen data, achieving 92.8% accuracy. This indicates the hybrid model assesses the left and right hands' ability to decode the MI signal. Consequently, The RF-VGG19 model can aid the BCI-MI community by simplifying the implementation of the mobile biometric authentication requirement, specifically in subject identification and lock and unlock classification.

## 1. INTRODUCTION

As an essential component of system security in the field of information systems, identity authentication is a crucial assurance. However, there are varying degrees of security concerns associated with classic biometric identification systems. For example, biometric data can be stolen or replicated [1, 2]. The scientific subject of IT security is expanding steadily, and as such, it needs to develop. It is a difficult task for security scientists from various fields of competence to collaborate and agree on methodologies, procedures, and outcomes because of its immense complexity and variety of viewpoints [3-5]. Information systems (IS) are increasingly indispensable in several domains of life for humans, ranging from the military to the healthcare business. Consequently, there is a growing imperative to ensure the security of IS. This is mainly due to the fact that computer systems store sensitive information, and without security, people and organizations are unable to share data or make use of the technology.[6]. Over the last few decades, the ability to automatically identify or authenticate people has been the focus of computer science research. This has involved interdisciplinary sciences collaborating to continuously develop automated methods that are more precise, quicker, more convenient, and less susceptible to impersonation[7]. Electroencephalogram (EEG) brain signals are used for an authentication process, according to research on brain biometrics. Potential uses for EEG data unique qualities for user authentication include the ability to discern between different brain processes. This approach is much more secure and resilient than other biometric systems since the answer is altered based on the user's instantaneous mental state[8, 9]. Furthermore, Due to its unique characteristics, EEG is superior to conventional biometric modalities like fingerprint and iris in terms of privacy compliance, robustness against spoofing assaults, and aliveness detection[10]. In electroencephalography (EEG) to other noninvasive brain signal acquisition models, recent research has demonstrated that EEG is a cost-effective, portable, and easy to use noninvasive technique for recording brain activity that can be used to develop biometric systems. An individual's EEG signals are recorded while they are in a comfortable resting state, with their eyes open or closed and experiencing active response stages. It has been noted that these signals are strong transmitters of distinct personality traits[11]. Electroencephalography (EEG) is a powerful brain imaging technique when compared to other functional neuroimaging methods like positron emission tomography (PET), magnetoencephalogram (MEG), functional magnetic resonance imaging (fMRI), and transcranial magnetic stimulation (TMS). These characteristics include mobility, safety, non-invasiveness, high flexibility, high temporal resolution, low cost, and ease of usage[12]. Compared to other biometric modalities, such as electrocardiography (ECG) and electromyography (EMG), electroencephalography (EEG) signals are more promising due to their rich dynamic properties and extremely high temporal resolution[10]. Electroencephalography (EEG) and motor imagery (MI) signals have garnered significant attention recently because they convey a person's intention to do an activity. Researchers have utilized MI signals to assist people with disabilities in controlling wheelchairs and other devices [13], Biomedicine [14] and even self-driving cars [15]. Additionally, they are used in [16]. To be more precise, MI is the name given to a particular type of cognitive activity in which a subject imagines moving their arms or legs but doesn't actually do so. When a movement is imagined, certain brain regions involved in its planning and execution must be consciously activated. This is usually done in conjunction with a willful effort to prevent the real movement from occurring[17, 18]. Decoding MI-EEG data is a very challenging endeavor due to its dynamic nature, poor signal-to-noise ratio, and complexity[19]. As a result, MI pattern identification systems require three critical procedures: EEG signal preprocessing, feature extraction, and classification[20]. In the MI-EEG pattern recognition approach, feature extraction is essentially the key procedure.

Particularly for classification, the use of time-frequency representation (TFR) to analyses motor imagery (MI) features is a widely used technique in brain-computer interface (BCI) applications. The aforementioned diagram illustrates the power and dispersion of signal energy throughout a wide range of time intervals and frequencies through the combination of functions of time and frequency [10][15]. Due to the fundamentally one-dimensional nature of the MI signal, it is necessary to convert it into two-dimensional images. This can be achieved by implementing the techniques of Continuous Wavelet Transform (CWT) and Short-Time Fourier Transform (STFT). The previously investigated techniques exhibit exceptional effectiveness and expertise in the administration of signal properties spanning both the temporal and frequency domains [11]. However, Electroencephalograms (EEGs) are frequently regarded as non-stationary signals in situations involving brief time intervals. In these conditions, the Short-Time Fourier Transform (STFT) methodology seems to be a feasible way to extract and calculate the time-frequency domain spectrum of the brain signal [12]. Furthermore, a benefit of the Short-Time Fourier Transform (STFT) technique is that it offers concurrent information in the time-frequency domain at a comparatively low computational expense [13][21]. In a similar manner it has also been demonstrated that the convolutional neural network (CNN) can extract temporal and spatial information from magnetic induction (MI) data. The results of previous research have demonstrated that convolutional neural networks (CNNs) have the potential to extract highly effective features from both shallow and deep models. This suggests that advantageous attributes may be produced at different levels of the network architecture [8][22]. Furthermore, the implementation of deep transfer learning methodologies streamlines the process of integrating new datasets into a pre-existing machine learning model. Because the

amount of data that is typically given is insufficient to guarantee that the model is properly trained, this feature is especially helpful for brain-computer interface (BCI) systems [14][23]. The results of the BCI research suggest that convolutional neural network (CNN)-based subject transfer methods outperformed alternative approaches. These subject-transfer approaches depend on the assumption that the typical patterns of the target subject and other subjects can be compared while performing the same activities [15][24]. The selection of a suitable classifier becomes crucial since it plays a significant role and directly affects the ability to distinguish between two MI-EEG mental commands. In order to accomplish classification, traditional machine learning techniques require the usage of manually created features. Nonetheless, categorization is carried out by deep convolutional neural networks (DCNN), which directly extract characteristics from unprocessed input[25, 26]. Previous studies, such as [27-29], have classified computer vision problems by combining a traditional machine learning approach with pretrained CNNs. Additionally, studies such as [30, 31] have identified seizures caused on by epilepsy using the same technique. The aim of this study is to utilize a hybrid approach that integrates pretrained Convolutional Neural Networks (CNNs) with a traditional machine learning method in order to decode two-class Motor Imagery (MI) signals for Electroencephalogram (EEG) biometric identification. EEG signals are caused by both imagined and actual human movement. In motor imaging, EEG data show synchronization (ERS) and desynchronization (ERD) properties[32]. In order to capture both ERS and ERD motor activity, a 4-second trial's 2D pictures, or spectrograms, are created using the STFT approach. This approach uses one EEG channel and produces six pictures related to the alpha and beta bands. Subsequently, The VGG-19 model is utilized to extract features from the motor imaging data, which are subsequently combined with the classifier to carry out the classification method [33]. The paper is organized as follows: Section 2 provides a brief summary of the technique; Section 3 expands on the results and comments; and Section 4 delivers the study's findings and conclusions.

## 2. METHODOLOGY

The hybrid model's methodology for MI signal decoding is illustrated in Figure 1. Sections that follow this framework's outline provide further detail on the concept and its implementation of the MI pattern detection technique:

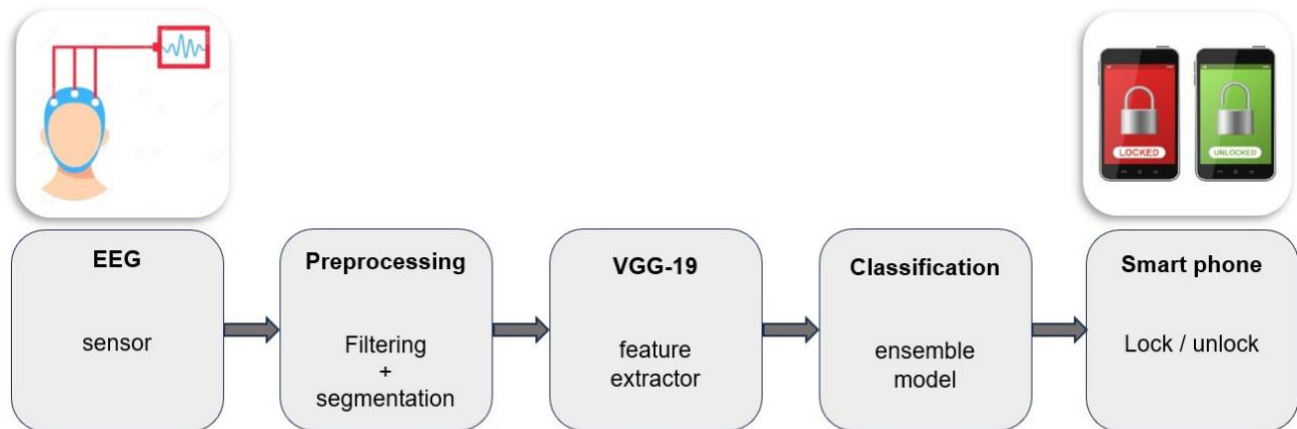


Fig .1. Methodological Framework for Ensemble Model

### 2.1 MI EEG Datasets

Developers of brain-computer interface (BCI) systems usually decide to use as few channels as possible. This strategy lowers the costs related to real-time applications and facilitates simpler deployment [14]. As a result, two MI EEG datasets with three channels of recording are chosen for this study. The study's two datasets came from the BCI competition datasets, which were collected at Graz University. The following subsections provide more information about the two datasets. The training and evaluation sections of the datasets are two distinct components. Consequently, the hybrid model was used to assess inter and intra-subject variances[34, 35]. Because a large dataset was not readily available, the datasets of the nine participants had to be combined in order to produce a single, comprehensive dataset that included all trials. This strategy was used to build a robust model that could successfully handle the complicated problems brought on by brain complexity.

## 1. Dataset-I (BCI IV 2b dataset)

The dataset consisted of three channels of electroencephalogram (EEG) data (C3, Cz, and C4), which recorded signals related to two separate motor imagery tasks: movements executed with the left and right hands. At a sample frequency of 250 Hz, the data was gathered from a group including nine different individuals. An electroencephalogram (EEG) was obtained from an individual who was put in an armchair and instructed to stare at a flat screen for the duration of 160 trials. There were two separate recording sessions: one for training with no feedback and the other for evaluation with positive feedback. In the initial two sessions, the participants were provided with a concise auditory signal in the form of a warning tone. Four seconds of motor imagining exercises were conducted by the subjects in response to this cue. Participating in a cognitive simulation of a specific movement guided by an auditory signal in the form of a pointing arrow displayed on a screen devoid of physical components was the objective of this task. During the subsequent three sessions, participants received comprehensive guidance on modifying the grey smiley feedback, which was positioned at the center of the monitor. Following the display of a brief auditory signal, individuals were instructed to shift the feedback left or right. The feedback, depicted as a smiling emoticon, is transmitted within a time span of four seconds. The smiling face turns green while it's heading in the right direction, but red when it's going the wrong way [15]. As shown in Figure 2:

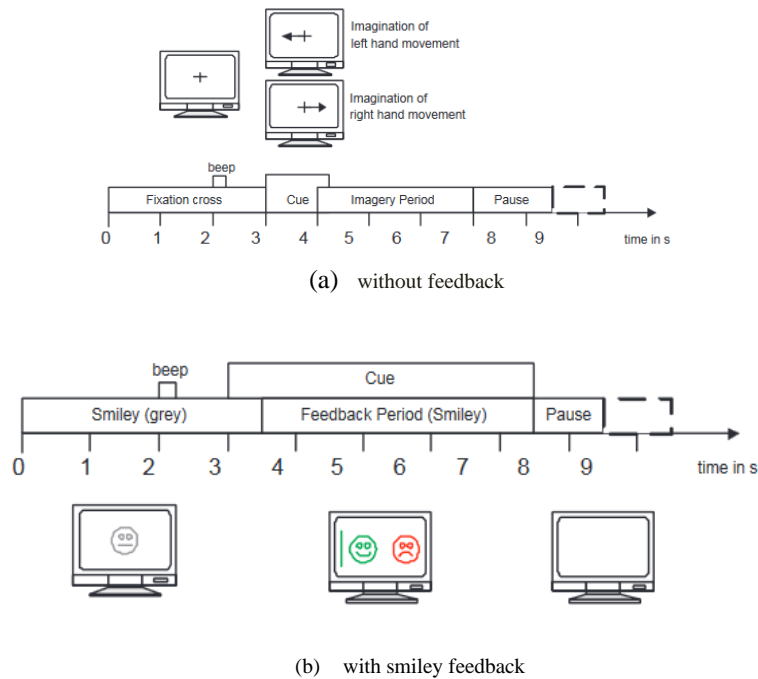


Fig .2. Trials Recording Time Scheme of the BCIC IV 2b Dataset

## 2. Dataset-II (BCI II dataset)

The dataset was collected from a singular participant, a healthy 25-year-old female. The sample frequency utilized by the electroencephalography (EEG) apparatus's three EEG channels (C3, Cz, and C4) was 128 Hz. The dataset was collected from a singular participant, a healthy 25-year-old female. The sample frequency utilized by the electroencephalography (EEG) apparatus's three EEG channels (C3, Cz, and C4) was 128 Hz.

The overall time for each trial is nine seconds. The grazing procedure was used to gather the dataset, and participants saw a period of quiet during the first two seconds. The experiment began with the presentation of a visual stimulus on the screen at the two-second mark. This was followed by the appearance of the cross symbol "+" for one second. At time  $t=3$  seconds, a visual stimulus in the shape of an arrow pointing to the right or left is displayed. The effectiveness of motor imagery in hand motions was assessed by the research through a thorough analysis that included 280 trials, with a focus on both left-

and right-hand movements. The dataset's whole signal is subjected to notch filtering between 0.5 and 30 Hz [16]. As shown in the Figure 3:

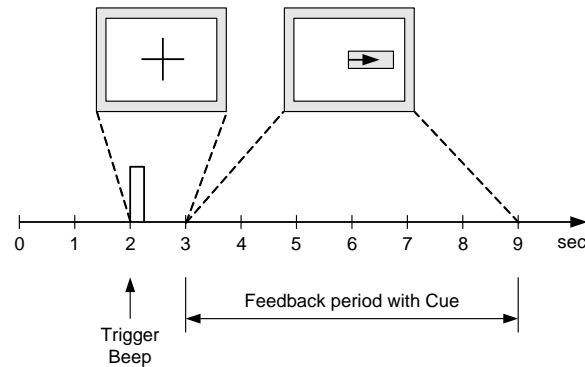


Fig .3. Trials Recording Time Scheme of the BCIC II Dataset

## 2.1 Pre-processing

The MI-EEG signal is contaminated by a number of factors, such as face muscle activity, eye blinking, body movements, and environmental artefacts such the electromagnetic fields generated by electrical gadgets [17]. Because deep learning is used within the framework, there is minimal preprocessing involved[36]. In order to enhance the signal-to-noise ratio of unprocessed EEG data and highlight pertinent information contained within the signals, frequency filtering is implemented. Since the alpha (8-13 Hz) and beta (14-30 Hz) rhythms are crucial to motor imagery (MI) electroencephalogram (EEG) data, fourth-order Butterworth filtering is employed in the 8-30 Hz frequency range.

### VGG-19

In order to accurately describe the latent characteristics of the brain signal in the context of the EEG signal classification problem, high-dimensional features are required. CNN employs many kernels, sometimes referred to as filters, in order to extract dominant features through the convolution process[25]. Transfer learning is the process of retraining a few of a previously trained network's final layers in order to answer a new categorization problem. This significantly reduces the number of training samples required and significantly saves time compared to training the network from the beginning. Karen Simonyan and Andrew Zisserman were the principal architects and developers of the pre-trained VGG framework. Using the ImageNet dataset, which comprises 14 million images with 1,000 distinct classifications, the model was trained. Because this deep learning framework demonstrated superior performance on two important computer vision issues, localization and classification, it was used in numerous research applications [37, 38]. To improve the feature extraction procedure, the VGG-19 version of the VGG architecture raises the kernel size from 64 to 512 [39, 40]. Essentially, the pooling layer, which has a stride size of 2x2, comes after the convolution layer unit. The downsampling in this network is accomplished using max-pooling, whereas the activation function utilised is the Rectified Linear Unit (ReLU). The input image has a resolution of 224 x 224 and is composed of three fully connected layers with varying layer orders, including 4096, 4096, and 1000. This CNN network's classification idea is predicated on the likelihood of applying the softmax to multiclass problems [41]. A VGG-19 model was used to extract features from motor imaging signals[40]. CNN-based biometric recognition achieved very high accuracy[33, 42]. Three layers make up the main components of the VGG-19: the convolution, pooling, and fully linked layers. Below is a description of this network in more detail:

- 1) The convolution layer: this layer is in charge of applying the filtering operation and performing the convolution operation on the input image in order to extract the feature map. This aids in comprehending a few elements and characteristics of the topographical image map. Local connection, which is enforced by the CNN network among neurons, aids in edge detection, sharpening, and blurring[43].
- 2) The Pooling layer: This layer is in charge of downsampling the feature map in order to reduce the features. This aids in controlling the issues with overfitting and underfitting. Depending on whether features are included in the patches, the typical pooling method is either average or max-pooling. In VGG-19, max pooling is most frequently employed[44].

- 3) The Fully Connected Layer, comprising three distinct layers, represents the ultimate component of the VGG-19. They take in information from the pooling and convolution layers, which are the preceding layers. This unit flattens its input before producing the final output by matrix multiplication carried out with a bias offset [45, 46].

## 2.2 Short Time Fourier Transform for EEG Image Formulation

Established by Gabor in 1946, the short-time Fourier transform (STFT) is a prevalent method in signal processing employed to analyse non-linear and non-stationary signals. It can define a raw signal's phase and magnitude, which vary with frequency and time [47]. It divides a long signal into equal-window segments and performs the Fourier transform on each segment [48]. This type of advanced Fourier analysis allows for a comprehensive estimation of a signal in both domains. The window function is employed by the Short-Time Fourier Transform (STFT) to extract a distinct subset of the time domain data for the purpose of identifying distinctive signal attributes. The cutout component is then subjected to the Fourier transform [49]. A brief time frame that moves along the time axis for STFT is multiplied by the processed EEG signal  $x(t)$ . A collection of windowed signal segments is the end outcome. Ultimately, The Fourier transform is utilized on individual segments of the signal that have been windowed, resulting in two-dimensional time-frequency spectrums of the original signal. The Short-Time Fourier Transform (STFT) is technically defined as follows [50]:

$$STFT(\tau, \omega) = \int_{-\infty}^{+\infty} dt w(t - \tau) e^{-i\omega t} dt \quad (1)$$

Equation (1) denotes a constant window size ( $w(t)$ ) and a finite number of non-zero values on the time axis ( $\tau$ ). By performing simultaneous analysis of the signal in both the temporal and frequency domains, the Short-Time Fourier Transform (STFT) technique makes it easier to evaluate the inherent properties of the EEG data that is incorporated. By denoting the raw MI signals for  $C$  channels and  $K$  samples as  $E = \{(X_i, y_i) | i = 1, 2, \dots, N\}$ , it is important to highlight that  $X_i \in \mathbb{R}^{C \times K}$  is a two-dimensional matrix that represents the  $i$ -th MI trial in the dataset. The dataset's total number of samples is indicated by the letter  $N$ . The labels for each  $X_i$  trial are represented by  $Y_i$ , and  $X_i$  stands for the total number of trials. The MI tasks for  $M$  classes are compromised since they get their values from the  $L$  set. There are two classes in total in this study, and they are designated with the labels  $L = \{l_1 = \text{"left"}, l_2 = \text{"right"}\}$ . Studies such as [51] demonstrated the STFT's effectiveness in producing 2D images (spectrograms) with a duration of 4 seconds, which were subsequently fed into CNN as input images. As a result, four seconds was selected as the duration, indicating that there was a total of 1,000 samples for each of the MI signals in the  $X_i$  experiment. Next, we decide on a 64-sample window size, of which 50 samples are overlapping. The result of this operation is an image that shows the values of each MI signal's power spectral density (PSD), expressed in Hertz. As a result, for every set of data obtained with three electrodes, three images are generated. However, For the purpose of recording the alpha and beta frequency bands, which are associated with the motor activity of the ERD and ERS, the present investigation generates six images for every MI trail.

## 3. RESULTS AND DISCUSSION

This section presents and discusses the results of the hybrid model's creation for biometric identification utilizing motor imagery. The results are provided and discussed. This model will be implemented for the mobile biometric authentication assignment, which consists of subject identification and lock/unlock classification. In essence, they give an account of the findings from six experiments. Building a hybrid model that might be used to the biometric authentication problem is the main goal of the first experiment. To complete this objective, nine hybrid models were built using nine different potential classifiers, most of which were well used classification techniques. The performance metrics of the models that were discussed earlier are presented in Table 1. The performance metrics indicate that the hybrid model incorporating both the RF classifier and AdaBoost classifier exhibits the highest level of performance. In particular, the model demonstrates a classification accuracy of 0.908 for the former, precision and recall of 0.908, area under the curve of 0.908, log loss of 1.134, specificity of 0.989, training time of 17:008, and testing time of 6.170. In terms of the latter, the classification accuracy is 0.912, F1=0.912, Precision=0.912, Recall=0.912, AUC=0.951, Log loss=3.033, Specificity=0.989, Training Time=56.252, and Testing Time=8.109. In relation to both training and testing time, when compared to the hybrid model that included the AdaBoost classifier, the performance of the RF-VGG19 model was significantly higher. As a result, the model that is often referred to as RF-VGG19 has been selected for use in mobile biometric authentication. A second experiment was conducted to evaluate how well the RF-VGG19 model identified participants.

TABLE 1. IDENTIFICATION OF TRAINING PART OVER DATASET-I.

Subjects	Performance Metrics								
	Training Time	Testing Time	AUC	CA	F1	Precision	Recall	Logloss	Specificity
Random Forest	17.008	6.170	0.977	0.908	0.908	0.908	0.908	1.134	0.989
AdaBoost	56.252	8.109	0.951	0.912	0.912	0.912	0.912	3.033	0.989
KNN	10.509	10.388	0.890	0.401	0.400	0.413	0.401	3.009	0.925
Tree	415.451	0.024	0.948	0.817	0.817	0.818	0.817	3.097	0.977
SVM	1100.967	183.904	0.899	0.574	0.569	0.594	0.574	1.543	0.947
SGD	96.079	13.831	0.907	0.834	0.834	0.834	0.834	5.730	0.979
Logistic Regression	380.585	9.074	0.903	0.571	0.571	0.572	0.571	1.251	0.946
Naive Bayes	15.692	4.027	0.765	0.351	0.355	0.376	0.351	20.488	0.919
Gradient Boosting	42058.514	6.339	0.985	0.903	0.903	0.904	0.903	0.597	0.988

		Predicted								
		Subject 1	Subject 2	Subject 3	Subject 4	Subject 5	Subject 6	Subject 7	Subject 8	Subject 9
Actual	Subject 1	1482	38	37	18	8	25	5	12	6
	Subject 2	20	1468	17	13	16	36	29	10	23
	Subject 3	28	24	1470	14	20	9	9	42	15
	Subject 4	9	5	5	1536	20	9	15	27	9
	Subject 5	20	16	29	15	1482	17	3	23	27
	Subject 6	27	45	12	15	19	1477	13	3	21
	Subject 7	15	33	9	23	8	12	1503	14	16
	Subject 8	17	11	31	33	21	19	6	1472	23
	Subject 9	21	22	12	11	33	15	30	28	1459

Fig .4. Confusion matrix for subject identification over the (Dataset-I)

Figure 2 serves as a visual representation of the outcome of the experiment that was mentioned earlier, more specifically the evaluation of Dataset I. The provided matrix is the confusion matrix generated during this test as shown in figure 4 and figure 5. The accuracy of the model's classification, the F1 score, the precision, the recall, and the area under the curve (AUC) are all 0.909, 0.909, 0.909, and 0.978, respectively. In terms of specificity, the value is 0.989, while the log loss is 1.082. The time required for training the model is 21.608, while the time required for testing it is 7.671. The third experiment evaluated the RF-VGG19 model's accuracy in subject identification. Within the context of this experiment, the confusion matrix that was utilized to evaluate Data Set I and Data Set II can be found in Figure 3. The accuracy of the presented model in terms of classification, the F1 score, the precision, the recall, and the area under the curve (AUC) are, respectively, 0.934, 0.934, 0.934, and 0.934. A log loss of 0.715 and a specificity of 0.993 are the results of the training and testing times, which are 23.910 and 8.571, respectively. The results of the three experiments that were conducted to identify subjects demonstrate that the RF-VGG19 model is capable of accurately identifying individuals based on the brain signals that they produce.

		Predicted									
		Subject 1	Subject 2	Subject 3	Subject 4	Subject 5	Subject 6	Subject 7	Subject 8	Subject 9	Subject10
Actual	Subject 1	1479	50	18	0	6	13	19	11	37	0
	Subject 2	45	1508	14	0	0	29	21	5	8	2
	Subject 3	32	28	1503	0	2	15	29	17	8	0
	Subject 4	0	0	0	1603	23	0	9	0	0	0
	Subject 5	12	0	8	42	1563	3	0	3	0	0
	Subject 6	42	69	34	0	3	1428	12	12	32	0
	Subject 7	25	21	18	0	0	17	1508	20	22	0
	Subject 8	20	29	15	0	3	12	21	1503	27	0
	Subject 9	20	28	3	0	14	21	11	9	1526	0
	Subject10	0	0	0	0	0	0	0	0	0	1430

Fig .5. Confusion matrix for subject identification over the (Dataset-I +Dataset-II)

The classification of lock and unlock tasks is the focus of the fourth experiment, which makes use of the RF-VGG19 conceptual framework. Nine individuals in total were included in the training parts of dataset I, which is where the experiment was carried out. This will enable the assessment of the model's capability to manage the complexities inherent in intra-subject brain signal complexity. Different subjects' brain signals vary in complexity. Table 2 outlines the experiment's results, which demonstrate that the nine participants had an average accuracy of 91.0% for the lock and unlock tasks.

TABLE II . VALIDATION OF RF-VGG-19 MODEL ON DATASET-I (TRAINING PART) FOR LOCK AND UNLOCK TASK

Subjects	Performance Metrics								
	Training Time	Testing Time	AUC	CA	F1	Precision	Recall	Logloss	Specificity
S1	10.379	5.314	0.986	0.940	0.940	0.941	0.940	0.220	0.940
S2	8.245	4.180	0.979	0.927	0.927	0.927	0.927	0.273	0.927
S3	8.045	4.470	0.980	0.929	0.929	0.929	0.929	0.236	0.929
S4	10.432	5.234	0.991	0.691	0.961	0.962	0.961	0.181	0.961
S5	10.217	5.413	0.982	0.932	0.932	0.933	0.932	0.232	0.932
S6	10.555	5.230	0.981	0.943	0.942	0.943	0.943	0.263	0.943
S7	11.144	5.445	0.983	0.938	0.938	0.939	0.938	0.243	0.926
S8	10.639	5.364	0.986	0.947	0.947	0.947	0.947	0.206	0.947
S9	9.879	5.754	0.986	0.951	0.951	0.951	0.951	0.238	0.951
Mean	9.948	5.156	0.983	0.910	0.940	0.941	0.940	0.232	0.939

Therefore, in the fifth experiment, the aim was to verify the efficacy of the RF-VGG19 model in the task of locking and unlocking. In the assessment phase, the experiment was run on dataset I. This will also help evaluate how well the model can address the problem of subjects' complicated brain signal changes. The findings of the experiment are presented in a simple and concise manner in Table 3, which gives the mean accuracy rates for the lock and unlock tasks across all nine individuals. A mean accuracy of 94.40% is achieved.

TABLE III. VALIDATION OF RF-VGG-19 MODEL ON DATASET-I (EVALUATION PART) FOR LOCK AND UNLOCK TASK

Subjects	Performance Metrics								
	Training Time	Testing Time	AUC	CA	F1	Precision	Recall	Logloss	Specificity
S1	10.638	5.357	0.984	0.943	0.943	0.943	0.943	0.227	0.943
S2	10.476	5.568	0.984	0.934	0.934	0.935	0.934	0.231	0.934
S3	8.325	4.107	0.987	0.945	0.945	0.946	0.945	0.221	0.945

S4	10.577	5.615	0.990	0.956	0.956	0.956	0.956	0.197	0.956
S5	10.870	5.453	0.985	0.941	0.941	0.941	0.941	0.221	0.941
S6	8.566	4.800	0.982	0.933	0.933	0.933	0.933	0.232	0.933
S7	8.643	4.762	0.981	0.935	0.935	0.936	0.935	0.286	0.935
S8	8.873	4.733	0.991	0.962	0.962	0.962	0.962	0.191	0.962
S9	8.141	4.240	0.987	0.949	0.949	0.949	0.949	0.210	0.949
Mean	9.456	4.959	0.985	0.944	0.944	0.944	0.944	0.224	0.944

The sixth experiment's main goal was to evaluate the RF-VGG19 model's performance in the lock and unlock task using a unique dataset that had never been seen previously. The dataset consists of two separate parts, the testing part and the training part, each containing data for a single person. The information in these two sections was acquired throughout the course of two distinct sessions. The results of the RF-VGG19 model for the classification accuracy on the training and testing parts are 0.916 and 0.928, respectively, as it is demonstrated in Table 4 with their respective performance metrics.

TABLE IV. FEMALE DATASET-II (TRAINING PART AND TESTING PART) RF CLASSIFICATION

	<i>Performance Metrics</i>								
	<i>Training Time</i>	<i>Testing Time</i>	<i>AUC</i>	<i>CA</i>	<i>F1</i>	<i>Precision</i>	<i>Recall</i>	<i>Logloss</i>	<i>Specificity</i>
<i>Dataset-II</i> Training Part	17.788	5.908	0.982	0.916	0.916	0.917	0.916	0.932	0.991
Testing Part	16.607	5.922	0.987	0.928	0.928	0.928	0.928	0.730	0.992

When comparing the RF-VGG19 model's accuracy to datasets I, it is clear that the model outperforms the present literature (Tables 5). The purpose of this study is to determine whether or not the suggested model is capable of recognizing brain signals that are associated with motor imagery in both the left and right hands. This study's findings might be useful for mobile biometric authentication systems that use facial recognition to identify users and classify their actions (such as lock and unlock). The BCI-MI community will gain substantial advantages from this hybrid model as it broadens the potential applications of the proposed model to include biometric authentication systems based on MI.

TABLE V. RESULTS COMPARISON WITH STATE-OF-ART STUDIES RELATED TO DATASET-I

<i>Year</i>	<i>Study</i>	<i>Method</i>	<i>Accuracy</i>
2015	[52]	LDA-based wrapper SFS	90%
2016	[53]	STFT with KNN	83.57%
2016	[54]	WT+SE using SVM and KNN	86.4%
2016	[55]	MEMD + STFT with KNN	90.71%
2017	[56]	Fuzzified Adaptation with SVM	81.48%
2019	[57]	Genetic Algorithm with FKNN	84%
2019	[48]	STFT with CNN	89.73%
2023	This Study	Proposed Method	91%,94%

#### 4. CONCLUSION

The present study attempted to use a traditional classifier and the hybridization technique with VGG-19. This technique, referred to as a hybrid model, was used for the mobile biometric authentication need to decode two class MI signals: the subject's identity as well as the classification of locks and unlocks. In order to accomplish this, nine hybrid models were created using nine possible classifiers, which were primarily well used classification techniques. The best model was then chosen. Sixth experiments were actually carried out in this study's experimental section. In order to solve the issue of biometric authentication, the first experiment will focus on developing a hybrid approach to the problem. Nine potential classifiers, or commonly used classification techniques, were employed to construct nine hybrid models in order to achieve this. It is evident that the RF-VGG19 model outperformed the other models in terms of performance. It was decided to employ it for mobile biometric authentication as a result. In the fourth trial, locks and unlocks are categorized using the

RF-VGG19 model, which has a mean accuracy of 91.0%. As a result, the validation of the RF-VGG19 model for the lock and release task was accomplished in the fifth experiment, which achieved an average accuracy of 94.40%. In actuality, in the sixth experiment, a separate dataset containing unseen data was used to validate the RF-VGG19 model's 92.8% accuracy for the lock and unlock task. They imply that the RF-VGG19 paradigm has the potential to benefit the BCI-MI community by simplifying the deployment of mobile biometric authentication (subject identification and lock/unlock classification).

### Conflicts Of Interest

The author's disclosure statement confirms the absence of any conflicts of interest.

### Funding

The author's paper does not provide any information on grants, sponsorships, or funding applications related to the research.

### Acknowledgment

The author acknowledges the support and resources provided by the institution in facilitating the execution of this study.

### References

- [1] S. Zhang, L. Sun, X. Mao, and P. Liu, "EEG topomap-based Identification scheme," in *2021 3rd International Academic Exchange Conference on Science and Technology Innovation (IAECST)*, 2021, pp. 287-293: IEEE.
- [2] O. S. Ojo, M. O. Oyediran, B. J. Bamgbade, A. E. Adeniyi, G. N. Ebong, and S. A. Ajagbe, "Development of an Improved Convolutional Neural Network for an Automated Face Based University Attendance System," *ParadigmPlus*, vol. 4, no. 1, pp. 18-28, 2023.
- [3] R. Andersson, "Evaluation of the security of components in distributed information systems," ed: Institutionen för systemteknik, 2003.
- [4] R. A. Hamid et al., "How smart is e-tourism? A systematic review of smart tourism recommendation system applying data management," *Computer Science Review*, vol. 39, p. 100337, 2021.
- [5] N. S. Baqer, H. A. Mohammed, A. Albahri, A. Zaidan, Z. Al-qaysi, and O. Albahri, "Development of the Internet of Things sensory technology for ensuring proper indoor air quality in hospital facilities: Taxonomy analysis, challenges, motivations, open issues and recommended solution," *Measurement*, vol. 192, p. 110920, 2022.
- [6] H. Mouratidis, P. Giorgini, and G. Manson, "When security meets software engineering: a case of modelling secure information systems," *Information Systems*, vol. 30, no. 8, pp. 609-629, 2005.
- [7] S. Puengdang, S. Tuarob, T. Sattabongkot, and B. Sakboonyarat, "EEG-based person authentication method using deep learning with visual stimulation," in *2019 11th International Conference on Knowledge and Smart Technology (KST)*, 2019, pp. 6-10: IEEE.
- [8] I. Jayarathne, M. Cohen, and S. Amarakeerthi, "BrainID: Development of an EEG-based biometric authentication system," in *2016 IEEE 7th Annual Information Technology, Electronics and Mobile Communication Conference (IEMCON)*, 2016, pp. 1-6: IEEE.
- [9] M. H. Jasim et al., "Emotion detection among Muslims and non-Muslims while listening to Quran recitation using EEG," *Int J Acad Res Bus Soc Sci*, vol. 9, p. 14, 2019.
- [10] M. Wang, J. Hu, and H. A. Abbass, "BrainPrint: EEG biometric identification based on analyzing brain connectivity graphs," *Pattern Recognition*, vol. 105, p. 107381, 2020.
- [11] K. P. Thomas and A. Vinod, "Toward EEG-based biometric systems: The great potential of brain-wave-based biometrics," *IEEE Systems, Man, and Cybernetics Magazine*, vol. 3, no. 4, pp. 6-15, 2017.
- [12] A. Khosla, P. Khandnor, and T. Chand, "A comparative analysis of signal processing and classification methods for different applications based on EEG signals," *Biocybernetics and Biomedical Engineering*, vol. 40, no. 2, pp. 649-690, 2020.
- [13] Z. Al-Qaysi, B. Zaidan, A. Zaidan, and M. Suzani, "A review of disability EEG based wheelchair control system: Coherent taxonomy, open challenges and recommendations," *Computer methods and programs in biomedicine*, vol. 164, pp. 221-237, 2018.
- [14] M. M. Salih, M. Ahmed, B. Al-Bander, K. F. Hasan, M. L. Shuwandy, and Z. Al-Qaysi, "Benchmarking Framework for COVID-19 Classification Machine Learning Method Based on Fuzzy Decision by Opinion Score Method," *Iraqi Journal of Science*, pp. 922-943, 2023.
- [15] Z. Al-Qaysi et al., "Systematic review of training environments with motor imagery brain-computer interface: coherent taxonomy, open issues and recommendation pathway solution," *Health and Technology*, vol. 11, no. 4, pp. 783-801, 2021.

- [16] A. B. Tatar, "Biometric identification system using EEG signals," *Neural Computing and Applications*, vol. 35, no. 1, pp. 1009-1023, 2023.
- [17] R. Das, E. Maiorana, and P. Campisi, "Motor imagery for EEG biometrics using convolutional neural network," in *2018 IEEE International Conference on Acoustics, Speech and Signal Processing (ICASSP)*, 2018, pp. 2062-2066: IEEE.
- [18] Z. Al-Qaysi et al., "A systematic rank of smart training environment applications with motor imagery brain-computer interface," *Multimedia Tools and Applications*, vol. 82, no. 12, pp. 17905-17927, 2023.
- [19] S. U. Amin, M. Alsulaiman, G. Muhammad, M. A. Mekhtiche, and M. S. Hossain, "Deep Learning for EEG motor imagery classification based on multi-layer CNNs feature fusion," *Future Generation computer systems*, vol. 101, pp. 542-554, 2019.
- [20] R. Liu, Z. Zhang, F. Duan, X. Zhou, and Z. Meng, "Identification of Anisomeric Motor Imagery EEG Signals Based on Complex Algorithms," *Computational intelligence and neuroscience*, vol. 2017, 2017.
- [21] R. A. Aljanabi, Z. Al-Qaysi, M. Ahmed, and M. M. Salih, "Hybrid Model for Motor Imagery Biometric Identification," *Iraqi Journal For Computer Science and Mathematics*, vol. 5, no. 1, pp. 1-12, 2024.
- [22] S. M. Samuri, T. V. Nova, B. Rahmatullah, S. L. Wang, and Z. T. Al-Qaysi, "Classification model for breast cancer mammograms," *IJUM Engineering Journal*, vol. 23, no. 1, pp. 187-199, 2022.
- [23] Z. Al-qaysi, A. Albahri, M. Ahmed, and M. M. Salih, "Dynamic decision-making framework for benchmarking brain-computer interface applications: a fuzzy-weighted zero-inconsistency method for consistent weights and VIKOR for stable rank," *Neural Computing and Applications*, pp. 1-24, 2024.
- [24] M. Ahmed, B. Zaidan, A. Zaidan, M. M. Salih, Z. Al-Qaysi, and A. Alamoody, "Based on wearable sensory device in 3D-printed humanoid: A new real-time sign language recognition system," *Measurement*, vol. 168, p. 108431, 2021.
- [25] T. Kaur and T. K. Gandhi, "Automated brain image classification based on VGG-16 and transfer learning," in *2019 International Conference on Information Technology (ICIT)*, 2019, pp. 94-98: IEEE.
- [26] M. Ahmed, Z. Al-Qaysi, M. L. Shuwandy, M. M. Salih, and M. H. Ali, "Automatic COVID-19 pneumonia diagnosis from x-ray lung image: A Deep Feature and Machine Learning Solution," in *Journal of Physics: Conference Series*, 2021, vol. 1963, no. 1, p. 012099: IOP Publishing.
- [27] Y. Mangalmurti and N. Wattanapongsakorn, "COVID-19 and Other Lung Disease Detection Using VGG19 Pretrained Features and Support Vector Machine," in *2021 25th International Computer Science and Engineering Conference (ICSEC)*, 2021, pp. 51-56: IEEE.
- [28] M. Ahmed, Z. Al-qaysi, M. L. Shuwandy, M. M. Salih, and M. H. Ali, "Automatic COVID-19 pneumonia diagnosis from x-ray lung image: A Deep Feature and Machine Learning Solution," in *Journal of Physics: Conference Series*, 2021, vol. 1963, p. 012099: IOP Publishing.
- [29] A. S. Albahri et al., "Role of biological data mining and machine learning techniques in detecting and diagnosing the novel coronavirus (COVID-19): a systematic review," *Journal of medical systems*, vol. 44, pp. 1-11, 2020.
- [30] A. Saidi, S. B. Othman, and S. B. Saoud, "A novel epileptic seizure detection system using scalp EEG signals based on hybrid CNN-SVM classifier," in *2021 IEEE Symposium on Industrial Electronics & Applications (ISIEA)*, 2021, pp. 1-6: IEEE.
- [31] S. Garfan et al., "Telehealth utilization during the Covid-19 pandemic: A systematic review," *Computers in biology and medicine*, vol. 138, p. 104878, 2021.
- [32] Z. Al-Qaysi, A. Al-Saegh, A. F. Hussein, and M. Ahmed, "Wavelet-based Hybrid learning framework for motor imagery classification," *Iraqi J Electr Electron Eng*, 2022.
- [33] M. Hadid, Q. M. Hussein, Z. Al-Qaysi, M. Ahmed, and M. M. Salih, "An Overview of Content-Based Image Retrieval Methods And Techniques," *Iraqi Journal For Computer Science and Mathematics*, vol. 4, no. 3, pp. 66-78, 2023.
- [34] Z. Al-Qaysi, A. Albahri, M. Ahmed, and S. M. Mohammed, "Development of hybrid feature learner model integrating FDOSM for golden subject identification in motor imagery," *Physical and Engineering Sciences in Medicine*, pp. 1-16, 2023.
- [35] A. Albahri et al., "A Trustworthy and Explainable Framework for Benchmarking Hybrid Deep Learning Models Based on Chest X-Ray Analysis in CAD Systems," *International Journal of Information Technology & Decision Making*, 2024.
- [36] O. Albahri et al., "Systematic review of artificial intelligence techniques in the detection and classification of COVID-19 medical images in terms of evaluation and benchmarking: Taxonomy analysis, challenges, future solutions and methodological aspects," *Journal of infection and public health*, vol. 13, no. 10, pp. 1381-1396, 2020.

- [37] N. Begum and M. K. Hazarika, "Maturity detection of tomatoes using Transfer Learning," *Measurement: Food*, p. 100038, 2022.
- [38] A. H. Alamoodi et al., "Sentiment analysis and its applications in fighting COVID-19 and infectious diseases: A systematic review," *Expert systems with applications*, vol. 167, p. 114155, 2021.
- [39] M. Ahmed et al., "Intelligent decision-making framework for evaluating and benchmarking hybridized multi-deep transfer learning models: managing COVID-19 and beyond," *International Journal of Information Technology & Decision Making*, 2023.
- [40] Z. Al-Qaysi, A. Albahri, M. Ahmed, and S. M. Mohammed, "Development of hybrid feature learner model integrating FDOSM for golden subject identification in motor imagery," *Physical and Engineering Sciences in Medicine*, vol. 46, no. 4, pp. 1519-1534, 2023.
- [41] Y. Xia, M. Cai, C. Ni, C. Wang, E. Shiping, and H. Li, "A Switch State Recognition Method based on Improved VGG19 network," in *2019 IEEE 4th Advanced Information Technology, Electronic and Automation Control Conference (IAEAC)*, 2019, vol. 1, pp. 1658-1662: IEEE.
- [42] M. Ahmed, M. D. Salman, R. Adel, Z. Alsharida, and M. Hammood, "An intelligent attendance system based on convolutional neural networks for real-time student face identifications," *Journal of Engineering Science and Technology*, vol. 17, no. 5, pp. 3326-3341, 2022.
- [43] S. Kavitha, B. Dhanapriya, G. N. Vignesh, and K. Baskaran, "Neural Style Transfer Using VGG19 and Alexnet," in *2021 International Conference on Advancements in Electrical, Electronics, Communication, Computing and Automation (ICAECA)*, 2021, pp. 1-6: IEEE.
- [44] N. Abuared, A. Panthakkan, M. Al-Saad, S. A. Amin, and W. Mansoor, "Skin Cancer Classification Model Based on VGG 19 and Transfer Learning," in *2020 3rd International Conference on Signal Processing and Information Security (ICSPIS)*, 2020, pp. 1-4: IEEE.
- [45] S. Mascarenhas and M. Agarwal, "A comparison between VGG16, VGG19 and ResNet50 architecture frameworks for Image Classification," in *2021 International Conference on Disruptive Technologies for Multi-Disciplinary Research and Applications (CENTCON)*, 2021, vol. 1, pp. 96-99: IEEE.
- [46] A. Albahri et al., "A systematic review of using deep learning technology in the steady-state visually evoked potential-based brain-computer interface applications: current trends and future trust methodology," *International Journal of Telemedicine and Applications*, vol. 2023, 2023.
- [47] C. Huang, Y. Xiao, and G. Xu, "Predicting human intention-behavior through EEG signal analysis using multi-scale CNN," *IEEE/ACM Transactions on Computational Biology and Bioinformatics*, vol. 18, no. 5, pp. 1722-1729, 2020.
- [48] T. H. Shovon, Z. Al Nazi, S. Dash, and M. F. Hossain, "Classification of motor imagery EEG signals with multi-input convolutional neural network by augmenting STFT," in *2019 5th International Conference on Advances in Electrical Engineering (ICAEE)*, 2019, pp. 398-403: IEEE.
- [49] S. Chaudhary, S. Taran, V. Bajaj, and A. Sengur, "Convolutional neural network based approach towards motor imagery tasks EEG signals classification," *IEEE Sensors Journal*, vol. 19, no. 12, pp. 4494-4500, 2019.
- [50] G. Xu et al., "A deep transfer convolutional neural network framework for EEG signal classification," *IEEE Access*, vol. 7, pp. 112767-112776, 2019.
- [51] A. Al-Saegh, S. A. Dawwd, and J. M. Abdul-Jabbar, "CutCat: An augmentation method for EEG classification," *Neural Networks*, vol. 141, pp. 433-443, 2021.
- [52] R. Masoomi and A. Khadem, "Enhancing LDA-based discrimination of left and right hand motor imagery: Outperforming the winner of BCI Competition II," in *2015 2nd International Conference on Knowledge-Based Engineering and Innovation (KBEI)*, 2015, pp. 392-398: IEEE.
- [53] T.-U. Jang, B. M. Kim, Y.-M. Yang, W. Lim, and D.-H. Oh, "Motor-imagery EEG signal classification using position matching and vector quantisation," *International Journal of Telemedicine and Clinical Practices*, vol. 1, no. 4, pp. 306-313, 2016.
- [54] A. B. Das and M. I. H. Bhuiyan, "Discrimination and classification of focal and non-focal EEG signals using entropy-based features in the EMD-DWT domain," *Biomedical Signal Processing and Control*, vol. 29, pp. 11-21, 2016.
- [55] S. K. Bashar and M. I. H. Bhuiyan, "Classification of motor imagery movements using multivariate empirical mode decomposition and short time Fourier transform based hybrid method," *Engineering science and technology, an international journal*, vol. 19, no. 3, pp. 1457-1464, 2016.
- [56] R. Chatterjee, T. Bandyopadhyay, D. K. Sanyal, and D. Guha, "Dimensionality reduction of EEG signal using fuzzy discernibility matrix," in *2017 10th International Conference on Human System Interactions (HSI)*, 2017, pp. 131-136: IEEE.

- [57] S. V. Eslahi, N. J. Dabanloo, and K. Maghooli, "A GA-based feature selection of the EEG signals by classification evaluation: Application in BCI systems," *arXiv preprint arXiv:1903.02081*, 2019.